

determined. The main inner group was found to have an energy of 159.7 ± 0.5 keV with a relative intensity of $\sim 99.92\%$ ($\log ft = 5.1$). The cascading gamma ray following the inner group was found to have an energy of 764.5 ± 0.5 keV. The $K/(L+M)$ ratio for the gamma transition is 7.5 ± 0.1 , which is in close agreement with the theoretical value predicted for a pure $E2$ transition.

The internal conversion coefficient was found to be $\alpha_K = (1.1 \pm 0.1) \times 10^{-3}$. This is somewhat lower than values which have been reported^{5,11} previously and is also in closer agreement with the value predicted¹⁰ by theory for a pure $E2$ transition. No evidence was found for an intensity of as much as 1% for an additional 752-keV gamma transition as reported⁴ by Cork *et al.*

Beta Decay of Li^9 †

DAVID E. ALBURGER

Brookhaven National Laboratory, Upton, New York

(Received 29 May 1963)

A beryllium "rabbit" irradiated with neutrons from the $t+d$ reaction was transferred repeatedly to remote scintillation detectors by means of a timed pneumatic system. The spectrum of beta rays emitted by the Be sample and detected by means of a Pilot-B scintillator displays a strong component with a half-life of ~ 1 sec and $\beta_{\text{max}} \sim 3.5$ MeV and a weaker component with a half-life of 0.19 ± 0.03 sec and $\beta_{\text{max}} = 13.5 \pm 0.3$ MeV. These activities are identified as He^6 from the $\text{Be}^9(n,\alpha)\text{He}^6$ reaction and as Li^9 from the $\text{Be}^9(n,p)\text{Li}^9$ reaction, respectively. A much weaker component is assigned to N^{16} resulting from oxygen in the sample. Beta rays in coincidence with neutrons detected in a second Pilot-B crystal have an end-point energy of 11.0 ± 0.4 MeV. The coincidence spectrum from the neutron-detecting crystal displays a principal component corresponding to a neutron energy of 0.7 ± 0.2 MeV and gives some evidence for neutrons having an energy of 3–4.5 MeV. From these data, together with a shape analysis of the beta-ray singles spectrum, it is deduced that Li^9 decays with a 25% branch to the ground state of Be^9 ($\log ft = 5.5 \pm 0.2$) and with a 75% branch mostly to the known 2.430-MeV level ($\log ft = 4.7 \pm 0.2$). Both $\log ft$ values require allowed transitions and are compatible with a probable shell-model spin-parity assignment of $\frac{3}{2}^-$ to Li^9 and with the tentative assignment of $\frac{3}{2}^-$ given previously to the 2.430-MeV level. The cross section for forming Li^9 with neutrons of about 15.5 MeV is ~ 0.7 mb.

INTRODUCTION

IT is known¹ that Li^9 will decay to Be^9 with the emission of beta rays and delayed neutrons having a half-life of 0.169 ± 0.003 sec. When the present work was begun the only information on the decay energy of this nuclide came from a measurement² of the threshold for the $\text{Be}^9(d,2p)\text{Li}^9$ reaction. This predicted a Li^9 - Be^9 mass difference of 14.1 ± 1 MeV. During the course of the present experiments it was learned that a magnetic-spectrograph analysis of the $\text{Li}^7(t,p)\text{Li}^9$ reaction had been carried out by Middleton.³ He obtained a ground-state Q value of -2.397 ± 0.020 MeV for this reaction which establishes the Li^9 mass excess as 27.624 ± 0.022 MeV and the Li^9 - Be^9 mass difference as 13.614 ± 0.022 MeV. It had been reported⁴ that Li^9 is formed in the $\text{Be}^9(n,p)\text{Li}^9$ reaction using $t+d$ neutrons and that beta rays of > 4 MeV are emitted. More recently Nefkens⁵

has found several beta-ray activities in the 320-MeV photon irradiation of B^{11} . All of these have end-points of 13.1 ± 0.5 MeV and one is assigned to Li^9 . Based on cross-section arguments Nefkens finds that Li^9 decays 50–70% to the ground state of Be^9 .

According to shell-model considerations⁶ the most likely spin-parity assignment to Li^9 is $\frac{3}{2}^-$. In his study of the $\text{Li}^7(t,p)\text{Li}^9$ reaction Middleton³ found that the angular distribution of the ground-state proton group is characteristic of double stripping and can be fitted by assuming a mixture of $L=0$ and 2. This is expected if Li^9 is $\frac{3}{2}^-$. Such an assignment would imply that Li^9 should decay by an allowed beta-ray transition to the $\frac{3}{2}^-$ ground state of Be^9 . Another possible decay mode would be to the 2.430-MeV level in Be^9 which has been given a tentative assignment¹ of $\frac{3}{2}^-$ and which is in the position expected⁶ for a $\frac{3}{2}^-$ level. Further confirmation of this assignment has been obtained recently by Edge and Peterson⁷ who showed from electron scattering experiments that the 2.430-MeV level is connected to the ground state by a magnetic transition, probably $M1$.

Earlier work⁸ carried out in this laboratory on the

† Work performed under the auspices of the U. S. Atomic Energy Commission.

¹ F. Aijzenberg-Selove and T. Lauritsen, Nucl. Phys. **11**, 1 (1959).

² W. L. Gardner, F. N. Knable, and B. J. Moyer, Phys. Rev. **83**, 1054 (1951).

³ R. E. Middleton (private communication).

⁴ D. E. Alburger, A. Elwyn, A. Gallmann, J. V. Kane, S. Ofer, and R. E. Pixley, Phys. Rev. Letters **2**, 552 (1959).

⁵ B. M. K. Nefkens, Phys. Rev. Letters **10**, 243 (1963).

⁶ D. Kurath, Phys. Rev. **101**, 216 (1956).

⁷ R. D. Edge and G. A. Peterson, Phys. Rev. **128**, 2750 (1962).

⁸ D. H. Wilkinson and D. E. Alburger, Phys. Rev. **113**, 563 (1959).

13.6-sec decay of Be^{11} demonstrated the usefulness of a simple scintillation counter system for measurements on high-energy beta-ray emitters. In those experiments a Pilot-B scintillator 3 in. in diameter and 2 in. thick was used to detect beta rays both singly and in coincidence with gamma rays observed by means of a NaI counter. A decay scheme was deduced in which the end-point energy of the ground-state beta-ray transition was measured as 11.48 ± 0.15 MeV. This is in agreement with a later measurement⁹ of the Q value for the $\text{Be}^9(t,p)\text{Be}^{11}$ reaction which predicts an end-point energy of 11.510 ± 0.015 MeV for Be^{11} . In the present work some of the techniques developed in the Be^{11} experiments have been applied to a study of the decay scheme of Li^9 .

EXPERIMENTAL METHODS

The detectors used in this work consisted of two Pilot-B scintillators, one of which was 4 in. in diameter by 3 in. thick and the other 3 in. in diameter by 2 in. thick. The larger crystal was tapered down to a 3-in. diam at one end and fitted onto a 3-in.-diam CBS type 7818 phototube. Two layers of 0.001-in.-thick Al foil covered the front surface. The thickness of this crystal corresponds to the full range of beta rays of about 15 MeV. The other crystal was similarly mounted. Output pulses from the photo tubes were fed to conventional amplifiers, coincidence circuits and pulse-height analyzers.

All of the samples were irradiated by neutrons having a mean energy of about 15.5 MeV emitted from a thick titanium-tritium target bombarded with 700-keV deuterons from the Van de Graaff accelerator. At the beam currents of 30–50 μA that were generally used the total emission of neutrons from the target was $\sim 10^{10}$ per sec. In order to eliminate the very high "beam-on" machine background in the control room a pneumatically operated interceptor removed the beam from the tritium target during the counting intervals.

The beryllium sample to be irradiated consisted of a rod 0.120 in. in diameter and $\frac{1}{2}$ in. in length weighing 171 mg. This was located inside a $\frac{3}{8}$ -in.-i.d. by $\frac{1}{4}$ -in.-o.d. Saran tube which allowed the sample to be transported approximately 15 ft from a position directly in front of the tritium target, through the shielding wall and into the control room where the detecting equipment was placed. A system of two tanks of nitrogen gas and two solenoid-operated valves moved the sample back and forth. At a pressure setting of 40 psi the sample moved from one end of the tube to the other in 0.25 sec. It was stopped at either end by a bumper consisting of a $\frac{1}{8}$ -in.-long steel insert backed by a 1.5-in.-long Teflon insert, both having small central holes allowing the passage of the gas exhaust. In the control room the Saran tube crossed the detecting system such that when the Be

sample stopped it was symmetrically situated with respect to the axis of the detectors.

Timing of the pneumatic transport system, the beam interceptor and the counting devices was carried out automatically by means of a 30-rpm clock motor coupled to a pair of cams and microswitches. At the beginning of each 2-sec cycle the timer initiated the movement of the rabbit from the tritium target towards the detector and simultaneously actuated the beam interceptor. The latter cut off the beam in about 0.1 sec. Counting was begun after arrival of the rabbit at the detector by unblocking the pulse-height analyzers. By making adjustments of the cam angles the delay and duration of the counting interval could be varied for the different experiments. At the end of the first second the timer returned the rabbit to the target and opened the beam interceptor for the next irradiation.

In the earlier Be^{11} experiments⁸ the energies of the various beta-ray groups were obtained by comparing with the 10.40-MeV beta rays emitted in the decay of 7.4-sec N^{16} . Since the Be^{11} decay energy has now been established with high accuracy by nuclear reaction measurements⁹ it was possible in the present work to use Be^{11} as a reference standard that is closer in energy to Li^9 than is N^{16} . A primary calibration sample was, therefore, made by packing 203 mg of boron crystals (free of oxygen—see footnote 4 in Ref. 8) inside a short length of $\frac{1}{8}$ -in.-i.d. by $\frac{1}{4}$ -in.-o.d. plastic tubing over a length of $\frac{1}{2}$ -in. so as to closely reproduce the source geometry of the measurements on the Be sample. For secondary calibrations an oxygen sample was made by packing 135 mg of LiOH inside a similar length of tubing. These samples were irradiated by the neutron source (for making either Be^{11} or N^{16} by n,p reactions), the Van de Graaff beam was turned off, the samples were carried in, placed in the standard position in front of the detecting crystal and then counted. Several types of plastic tubing were tried before one was found (Samuel Moore Company type " p " tubing) that yielded no observable activity when a blank was irradiated and counted following the normal experimental procedure. For both Be^{11} and N^{16} the time from "beam-off" to the start of counting was about 9 sec. Most of the "singles" beta-ray spectrum measurements were made with the 4-in. \times 3-in. crystal.

Measurements of the coincidence spectra of both the beta rays and neutrons from Li^9 were made by using the two Pilot-B crystals. In order to achieve high efficiency the neutrons were detected in the larger crystal and the beta rays were detected in the smaller crystal. The two detectors were placed on opposite sides of the Saran pneumatic transport tube, the larger crystal being separated from the tube by sufficient thicknesses of various materials to absorb the beta rays. Each of the crystal outputs was fed to a separate 400-channel RIDL pulse-height analyzer and both analyzers were gated by the same pulses from a 0.1- μsec coincidence unit.

⁹ D. J. Pullen, A. E. Litherland, S. Hinds, and R. Middleton, Nucl. Phys. **30**, 1 (1962).

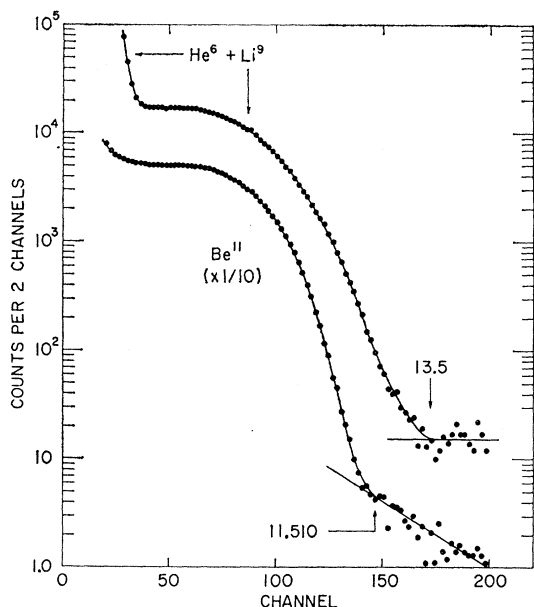


FIG. 1. Upper curve: spectrum of beta rays from a Be sample irradiated with $t+d$ neutrons and counted by means of a 4-in.-diam by 3-in.-thick Pilot-B scintillator. Lower curve: beta-ray spectrum of Be^{11} .

As an aid in interpreting the pulse-height distribution from the neutron-detecting crystal this detector was moved to a position 20 in. from the tritium target at 0° to the beam. An unused Zr-T target having a thickness of 0.5 mg/cm² was installed on the beam pipe and bombarded with a low-current beam of protons of various energies so as to yield monoenergetic neutrons of known energies. The pulse-height spectra were recorded for several neutron energies. In order to adjust the overall gain of the detecting system so as to be the same in this position as in the Li^9 coincidence runs a source of Bi^{207} was placed at the center of the crystal and the peak resulting from the 570-keV gamma rays and internal conversion electrons was centered at a reference channel number in each of the two experimental positions. This source was also used to adjust the timing of the coincidence circuit by observing the 1.06–0.57-MeV cascade transitions.

EXPERIMENTAL RESULTS

The upper curve in Fig. 1 shows the beta-ray spectrum following neutron irradiation of the Be sample and observed in the 4-in.-diam by 3-in.-thick Pilot-B crystal. This is the sum of three runs totaling 2 h and 40 min with a deuteron beam current of 46 μA on the tritium target. In each of the irradiate-count cycles the counting interval was 0.25 sec in duration beginning 0.25 sec after the cessation of the irradiation. In the lower part of Fig. 1 is a Be^{11} spectrum from irradiation of the boron sample. This was obtained by summing three sets of 4-min runs interlaced with the runs on the Be sample.

The procedure for the Be^{11} was to irradiate the boron sample for 30 sec, turn off the beam, carry the sample to the detector and then count for 30 sec. This was repeated until 4 min of counting had been reached.

It is evident that the spectrum from the Be sample consists of two major groups of particles. The lower energy but more intense component, only the tail of which is shown in the figure, has an end-point energy of about 3.5 MeV. In order to determine the end point of the higher energy group the channel number where the high-energy tail tapers into the background was compared with the corresponding channel number for the Be^{11} curve, as shown in Fig. 1. By using 11,510 MeV as the end-point energy of Be^{11} the Li^9 end-point energy is found to be 13.5 ± 0.3 MeV. It may be noted here that the technique that had been used⁸ in comparing Be^{11} with N^{16} was not suitable for the Li^9 - Be^{11} analysis. The Be^{11} - N^{16} comparisons had consisted of making an appropriate normalization of the intensities of the two spectra and then finding the ratios of channel numbers at fixed ordinate values over a region within a few MeV of the end point. These ratios were taken to be proportional to the ratio of end-point energies. In that case the shapes of the two spectra were quite similar and furthermore from the accuracy with which the decay schemes were known the normalization could be established well enough so that the error in the normalization did not introduce much error in the end-point determination. However, in the Li^9 - Be^{11} comparisons the shapes of the two spectra differ appreciably—presumably because of the large beta-ray branching of Li^9 to excited states, as discussed later, and it was not possible to fix the relative intensity of the ground-state group and, therefore, its normalization to Be^{11} with sufficient accuracy.

In order to check the validity of the present method of end-point analysis for the source shapes, counting geometry and crystal size used in this work, comparison measurements were made between N^{16} and Be^{11} . In the N^{16} runs the LiOH sample was irradiated for 15 sec and then counted for 15 sec and this procedure was repeated until the desired length of counting was reached. Within errors of about 0.2 MeV the correct ratio of end-point energies was obtained for N^{16} and Be^{11} . No corrections were made here or in the Li^9 - Be^{11} comparisons for the energy loss of beta rays due to sample size and wall thickness of the tubing. For all three samples the energy loss was estimated to be approximately the same, amounting to a few hundred keV. While this is a different fraction of the end-point energies of N^{16} , Be^{11} , and Li^9 the effect of neglecting the correction is small in comparison with the other errors. Measurements on the Be^{11} spectrum when using various source strengths showed that there were no appreciable count-rate gain shift or pile-up effects on the position of the end point.

The lifetime characteristics of beta rays from the Be sample were studied in several ways. Under the normal cycling conditions measurements of the spectrum were

made for various time delays of a 0.25-sec counting interval with respect to the cessation of irradiation. In one series of runs four spectra were recorded, each for the same number of irradiate-count cycles at a fixed beam current but with the counting interval at successive spacings of 0.1 sec. It was found that all four spectra could be nearly superposed within the statistics over the region above channel 40 (see Fig. 1) by adjusting their ordinates. The decrease of intensity of the spectrum with time delay corresponded to a half-life of 0.19 ± 0.03 sec.

The region of the strong component below channel 40 decayed very little over the 0.3-sec span used for these lifetime measurements. However, there was sufficient decay to be able to say that the half-life of that group is ~ 1 sec. Single irradiations followed by observation of the counting rate showed that most of the yield of the entire spectrum was gone within 5 sec. Although both the end-point energy and lifetime measurements on the lower energy component were rather rough it is very likely that this activity is associated with the decay of He^6 produced by the $\text{Be}^9(n,\alpha)\text{He}^6$ reaction (Q value -0.628 MeV). The accepted¹ end-point energy of He^6 is 3.536 MeV and its half-life is 0.813 sec.

When making these single irradiations of the Be sample it was noticed that not all of the yield above channel 40 had decreased to the very small normal background even after a few seconds. In order to investigate the origin of these longer lived beta rays the timer was operated by hand in such a way as to introduce a delay of 2 sec after irradiation, so as to allow the Li^9 to decay to negligible proportions, followed by 15 sec of counting. It then became apparent that the background had the characteristic end point of N^{16} . This was checked by a rough measurement of the rate of decrease of the counting rate integrated above channel 40. These results were consistent with the 7.4-sec half-life of N^{16} . It was concluded that the Be sample must contain a small amount of oxygen. Three other samples of Be metal also exhibited the N^{16} spectrum, whereas a sample of beryllium crystal irradiated with the $t+d$ neutrons showed $< 1/20$ as much N^{16} as did a Be metal sample of the same weight. It was then learned from the Metallurgy Group (Nuclear Engineering Department) of this Laboratory that all common samples of Be metal, in fact, contain a few tenths of a percent of oxygen.

In order to determine the fractional contribution of N^{16} to the spectrum shown in Fig. 1 a run was first made with 0.265-sec counting intervals beginning 0.25 sec after the end of irradiation, followed by a run that was the same in all respects except that the counting intervals were 0.70 sec in duration. The number of counts between channels 50 and 70 were summed in each case. For the 0.70-sec counting intervals the yield of Li^9 should be 1.42 times as much as for the 0.265-sec intervals (based on a half-life of 0.169 sec), whereas the N^{16} contribution should be 2.65 times greater. The

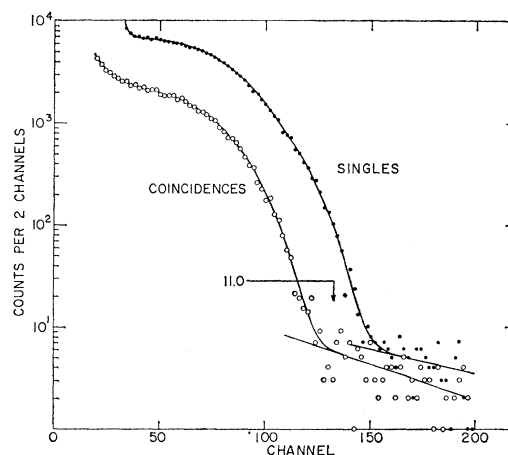


Fig. 2. Lower curve: spectrum of Li^9 beta rays entering a 3-in.-diam by 2-in.-thick Pilot-B crystal and in coincidence with neutrons detected by a 4-in.-diam by 3-in.-thick crystal, the latter being separated from the source by $\frac{1}{2}$ in. of brass. Upper curve: singles beta-ray spectrum from the Be sample. (Note the gain setting was different from that of Fig. 1.) The end point of the coincidence spectrum was obtained by a comparison with Be^{11} .

average experimental ratio of yields from two sets of runs was 1.49. It was calculated from this that about 6% of the yield between channels 50 and 70 in Fig. 1 was due to N^{16} . The presence of N^{16} probably explains why the 0.19-sec half-life value for Li^9 found in the measurements described previously was slightly higher than the accepted value of 0.169 sec.

The spectrum of beta rays which entered the 3-in.-diam by 2-in.-thick Pilot-B crystal and were in coincidence with the ungated output of the 4-in.-diam by 3-in.-thick crystal (shielded from beta rays by $\frac{1}{2}$ in. of brass) is shown together with the singles beta-ray spectrum in Fig. 2. These data represent the sums of six interlaced runs totaling 3 h on coincidences and 1 h on singles. If these data are analyzed by comparing their end points, as discussed in the analysis of Fig. 1, an energy separation of 2.2 MeV between the singles and coincidence end points would be indicated. However, because of the high energy of the ground-state beta-ray group and the possible distortion of its spectrum when measured in the 2-in. \times 3-in. crystal it was considered more reliable to compare the Li^9 coincidence spectrum with the singles spectrum of Be^{11} . This comparison, following the methods discussed for Fig. 1, results in a value of 11.0 ± 0.4 MeV for the end point of the Li^9 coincidence spectrum shown in Fig. 2.

In separate runs the pulse-height spectrum of the 4-in. \times 3-in. Pilot-B crystal was recorded in coincidence with the 3-in. \times 2-in. crystal output when the latter was biased to accept pulses above the He^6 end point (see Fig. 1). The spectrum obtained in a 6-h run is shown in the lower part of Fig. 3. For comparison the pulse-height spectra in the upper part of Fig. 3 were taken at the same gain but for monoenergetic neutrons incident on the crystal from the $\text{H}^3(p,n)\text{He}^3$ reaction at

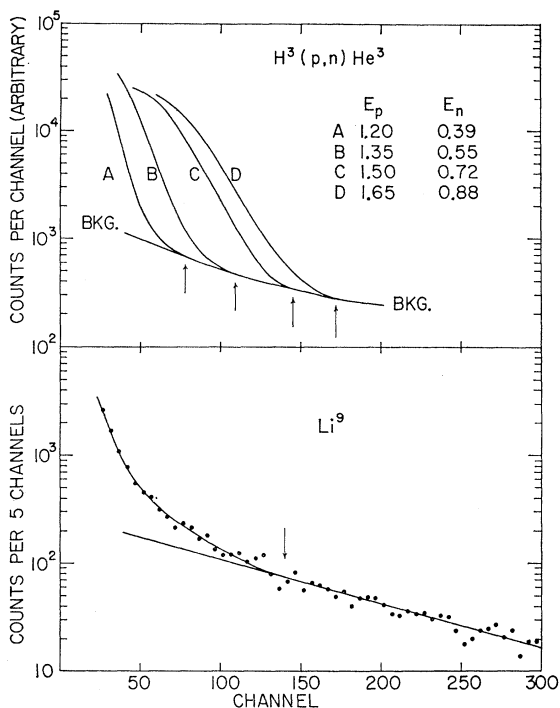


FIG. 3. The lower curve shows the pulse-height spectrum from the 4-in. \times 3-in. Pilot-B crystal (separated from the sample by beta-ray absorbers) in coincidence with Li^9 beta rays detected in a 3-in. \times 2-in. crystal when imposing a bias just above the He^6 end point. (See Fig. 1.) The upper curves are the spectra for the monoenergetic neutrons indicated.

four proton energies from 1.20 to 1.65 MeV yielding neutron energies at 0° of 0.39 to 0.88 MeV given in the figure. Because of the good statistics the data points have been omitted. Each of these curves displays a characteristic end point where the net yield tapers into the room background curve as determined with the beam off. The four curves have been matched along the room background curve and the end points indicated by arrows in the figure were estimated by eye. When plotted against neutron energy the end-point channel numbers fit quite well to a straight line passing through the origin.

Several tests were made for the possible presence of coincidence effects in the Li^9 spectrum of Fig. 3 other than beta-neutron coincidences. It was first shown that the entire distribution was associated with the irradiated Be sample and that the random coincidence contribution was completely negligible. Coincidences between beta rays and inner or outer bremsstrahlung were suspected. Outer bremsstrahlung could come from the beta-detecting crystal or from the absorber between the sample and the neutron-detecting crystal. In the latter case the bremsstrahlung would be in coincidence with back-scattered beta rays and the intensity of this effect would depend on the Z of the absorber. Spectra were run for brass, Al and Be absorbers but the shape of the curve was the same in all cases. Since the 570-keV Bi^{207}

reference line used for setting the gain was arbitrarily centered at channel 265 it is seen that the bulk of the coincidence spectrum of Fig. 3 is below an energy for electron response of 0.5 MeV. Thus, a further test was to use an absorber consisting of a sandwich of three $\frac{1}{4}$ -in.-thick plates of aluminum, brass, and lead with the Al next to the irradiated sample. If any major portions of the coincidence spectrum had resulted from bremsstrahlung it was expected that the lead absorber would modify the form of the spectrum considerably. However, in a coincidence run having comparable statistics the spectrum when compared with Fig. 3 was indistinguishable. One further effect might be beta-gamma coincidences associated with N^{16} or some other contaminant, although the shape of the spectrum is not at all what one would expect for gamma rays. In order to eliminate the beta-gamma coincidences from the N^{16} contaminant known to be present the bias on the beta-detecting crystal was increased to a point well above the 4.27-MeV end point of N^{16} beta rays leading to the 6.13-MeV level of O^{16} . No change in the shape of the coincidence spectrum was observed.

It was concluded from the above tests and from the shape of the coincidence spectrum that the entire distribution is very probably produced by neutrons and that at least two components are present. By estimating the end point of the lower-energy group (indicated by the arrow) in the same way as for the calibration curves a neutron energy of 0.7 ± 0.2 MeV is obtained. The higher energy distribution has a total intensity 5–10% as great as the low-energy group, depending on how the extrapolations back to the origin are made. One additional run was made at half the gain in an attempt to obtain the end point of the higher energy group. It was found that the yield flattened off to a very low, but apparently constant background level in a region corresponding to neutrons of between 3 and 4.5 MeV.

DISCUSSION

Except for the small N^{16} contamination mentioned previously, the beta rays above channel 40 in Fig. 1 have been assigned to Li^9 not only because the end-point energy of 13.5 ± 0.3 MeV agrees well with the reaction Q -value determination³ of 13.614 MeV for the $\text{Li}^9\text{-Be}^9$ mass difference, but because the decay measurements are consistent with the known half-life of that isotope. No known activities other than He^6 and Li^9 can be induced in Be by ~ 15.5 -MeV neutrons. For example, the production of Li^8 by the $\text{Be}^9(n,d)\text{Li}^8$ reaction (Q value -14.66 MeV) is not possible because the threshold for that reaction is above 16 MeV.

The coincidence work on Li^9 has established that there are relatively intense beta rays feeding excited states in Be^9 that decay by neutron emission. By comparing the coincidence beta-ray end-point energy of 11.0 ± 0.4 MeV with the singles end-point energy of 13.5 ± 0.3 MeV an excitation energy of 2.5 ± 0.5 MeV

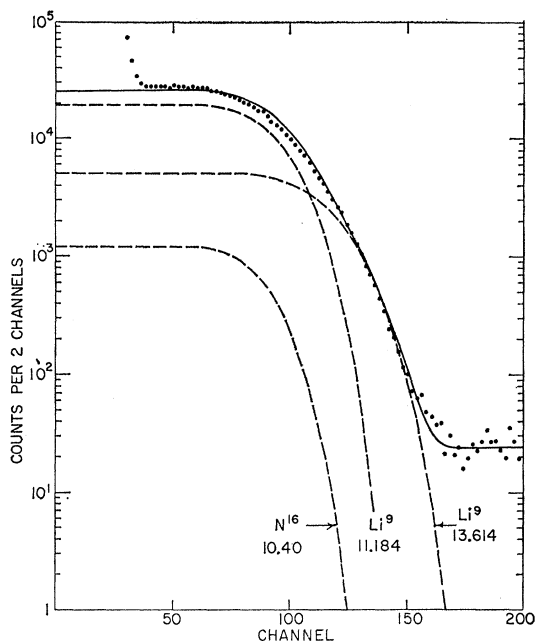


FIG. 4. Shape analysis of the Li^9 beta-ray spectrum in order to obtain the branching ratios. The dashed curves were constructed from the shape of the Be^{11} ground-state beta-ray spectrum and their sum (solid curve) gives the best fit to the experimental points.

in Be^9 is indicated. Alternatively, a comparison of the 11.0-MeV end point with the Li^9 - Be^9 mass difference of 13.614 MeV based on reaction Q values indicates a Be^9 excitation energy of 2.6 ± 0.4 MeV. Either of these results agrees best with the energy of the well-established Be^9 level¹ at 2.430 ± 0.002 MeV.

The lower energy component in coincidence with beta rays in Fig. 3, which corresponds to neutrons of 0.7 ± 0.2 MeV, could be associated only with the 2.430-MeV Be^9 level. Since this level is 0.763 MeV above $\text{Be}^8 + n$, one would expect the neutrons to have an energy of 0.68 MeV (allowing for recoil) provided that the decay proceeds by neutron emission to the ground state of Be^8 rather than going via $\text{Be}^9(2.430) \rightarrow \text{He}^4 + \text{He}^5 \rightarrow 2\text{He}^4 + n$. The present results are consistent with the emission of neutrons to the ground state of Be^8 .

Under the assumption that Li^9 decays only to the ground state of Be^9 and to the 2.430-MeV level an attempt was made to establish the branching ratios. In principle, this could be done from the ratio of the coincidence-to-singles beta-ray counting rates except that the neutron-detecting efficiency is not known accurately. It was felt that a shape analysis of the Li^9 singles spectrum would probably give a more reliable measure of the branching ratios. In order to do this a "standard" 11.51-MeV beta-ray spectrum was first derived. Following the procedure described in Ref. 8 the "standard" spectrum was obtained by subtracting from the total Be^{11} curve shown in Fig. 1 the 9.38-MeV component leading to the 2.13-MeV level of B^{11} , and

also by subtracting the extrapolated background near the end point. The abscissas of this net spectrum were then scaled up by a factor of $13.614/11.51$ and down by a factor of $11.18/11.51$ in order to obtain two separate spectra corresponding to the branches occurring in the decay of Li^9 . A third component corresponding to N^{16} was similarly constructed by using a scaling factor of $10.40/11.51$. The Li^9 constructed curves were then added together in various proportions and the N^{16} component was adjusted to be 6% of the total in order to correspond to the experimental determination of the relative intensity of this contamination. Near its end point the constructed curve was modified by adding on a background consistent with the relative level of the background beyond the end point of the experimental spectrum. Figure 4 shows the total constructed curve (solid line) obtained by summing the three components (dashed lines) and the background so as to give the best fit to the experimental points. Although there are slight differences between the constructed curve and the experimental points the agreement is probably as good as could be expected in view of the assumption that the various components have the same shape except for the scaling factor. It may be noted that the agreement would be better if a third beta-ray branch of lower end-point energy were assumed to be present in Li^9 decay.

The areas under the 13.614- and 11.18-MeV constructed components shown in Fig. 4 correspond to intensities of (25 ± 15) and $(75 \pm 15)\%$ for the branches to the ground state and to the 2.430-MeV level. Errors have been assigned so as to cover the possible inaccuracies in the shape analysis. $\log ft$ values for the branches obtained in this way are 5.5 ± 0.2 for the ground-state group and 4.7 ± 0.2 for the branch to the 2.43-MeV level. Both $\log ft$ values require allowed transitions. Since the ground state of Be^9 has a spin parity of $\frac{3}{2}^-$ the results are compatible with the shell-model prediction of $\frac{3}{2}^-$ for the spin parity of Li^9 and

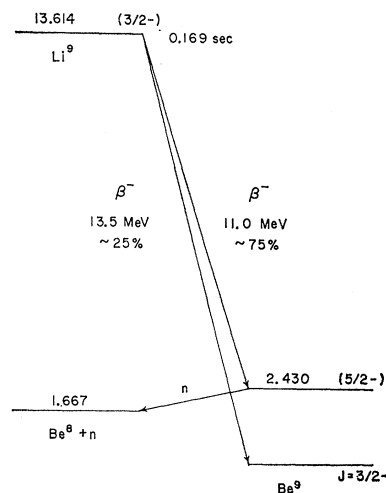


FIG. 5. Proposed decay scheme of Li^9 . The beta-ray energies and branching ratios are from the present work. Other information is from the literature (Ref. 1) except for the 13.614-MeV decay energy of Li^9 which is due to Middleton (Ref. 3). Evidence suggesting beta-ray branching to higher neutron-emitting states of Be^9 is presented in the text.

with the tentative assignment¹ of $\frac{5}{2}^-$ to the 2.430-MeV level.

The proposed decay scheme of Li^9 is shown in Fig. 5. Although the coincidence data of Fig. 3 strongly suggest that Li^9 also populates higher excited states in Be^9 that emit neutrons which may have energies as high as 4.5 MeV these results are not considered to be conclusive. In order to obtain more information on beta-ray branching to such states in Be^9 it would be useful to study the energy spectrum of the Li^9 neutrons in more detail. This might be done by means of a beta-neutron time-of-flight technique following the procedures used recently by Gilat, O'Kelley, and Eichler¹⁰ in a study of neutrons from N^{17} .

A calculation of the cross section for forming Li^9 at $E_n=15.5$ MeV was made by comparing the intensity

of the Li^9 beta-ray spectrum with that of N^{16} . At this neutron energy the cross section for the $\text{O}^{16}(n,p)\text{N}^{16}$ reaction is close to 30 mb as determined by DeJuren, Stooksberry, and Wallis.¹¹ By taking into account the relative numbers of O^{16} and Be^9 atoms in the two samples and the transport and counting times a cross section of 0.7 mb ($\pm 50\%$) is found for the formation of Li^9 in the $\text{Be}^9(n,p)\text{Li}^9$ reaction using neutrons having an average energy of about 15.5 MeV. This result agrees the previous estimate⁴ of ~ 0.6 mb for neutrons of the with same energy.

The author is indebted to Dr. B. M. K. Nefkens for suggesting this problem, to Dr. D. H. Wilkinson for helpful discussions, and to Dr. R. E. Middleton for communicating his unpublished results on the $\text{Li}^7(t,p)\text{Li}^9$ reaction. The pneumatic transport system was designed by Robert A. Lindgren.

¹⁰ J. Gilat, G. D. O'Kelley, and E. Eichler, *Bull. Am. Phys. Soc.* **8**, 320 (1963).

¹¹ J. A. DeJuren, R. W. Stooksberry, and M. Wallis, *Phys. Rev.* **127**, 1339 (1962).

Beta Decay of $\text{Li}^{8\dagger}$

D. E. ALBURGER

Brookhaven National Laboratory, Upton, New York

P. F. DONOVAN

Bell Telephone Laboratories, Murray Hill, New Jersey

and

Brookhaven National Laboratory, Upton, New York

AND

D. H. WILKINSON

Brookhaven National Laboratory, Upton, New York

and

Nuclear Physics Laboratory, Oxford, England

(Received 29 May 1963)

The beta decay of Li^8 , formed in the $\text{Li}^7(d,p)\text{Li}^8$ reaction, has been studied by measuring the energy distribution of the alpha particles that come from the subsequent breakup of Be^8 . The effects of the penetration into backing foils of the Li^8 recoils have been corrected for by comparing, for several deuteron bombarding energies, the alpha-particle spectra seen using a very thin foil target and the same target backed by a thick foil. The resulting "correct" alpha-particle spectrum is adjusted for various small effects including that due to electron-neutrino recoil and then compared with a prediction based on the empirical alpha-alpha scattering phase shifts, themselves adjusted by the subtraction of a hard-sphere phase shift. It is shown that the prediction is rather insensitive to the choice of hard-sphere radius. The agreement between the beta-decay data and the alpha-alpha phase shifts in the peak position (the "2.9-MeV state" of Be^8) is excellent as it is also in the shape of the transition probability distribution on the low- (alpha-particle) energy side of the peak where the falloff of intensity is here experimentally followed over two orders of magnitude. On the high-energy side of the peak, the familiar discrepancy is found in the sense that the transition probability is much too high to be explained by the first excited state alone. The present results, in addition to constituting an accurate comparison between Li^8 beta decay and alpha-alpha scattering, strengthen the interpretation of the reaction $\text{Be}^8(p,d)\text{Be}^8$ in terms of the "ghost" of the ground state of Be^8 and provide necessary data for discussing Li^8 and B^8 decay to regions of higher excitation in Be^8 where the effects of transitions to the tail of the first $T=1$ state of Be^8 are probably important.

INTRODUCTION

THE history of the excited state structure of Be^8 below the first $T=1$ state at about 17 MeV is a

[†] Work performed under the auspices of the U. S. Atomic Energy Commission.

complicated one. Over the years, many levels have come and gone but for some time now we have believed the true situation to possess the simplicity expected of it on either the independent-particle model or the alpha-particle model, namely, the $J^\pi=0^+$ ground state fol-